AP-Magazine-Revised-Tornero

Data · January 2016

CITATIONS
0

READS
147

5 authors, including:

José Luis Gómez Tornero
Universidad Politécnica de Cartagena
256 PUBLICATIONS **2,343** CITATIONS
SEE PROFILE

David Cañete Rebenaque
Universidad Politécnica de Cartagena
105 PUBLICATIONS **579** CITATIONS
SEE PROFILE

Fernando Daniel Quesada Pereira
Universidad Politécnica de Cartagena
171 PUBLICATIONS **675** CITATIONS
SEE PROFILE

P.A.M.E.L.A: A Useful Tool for the Study of Leaky-Wave Modes in Strip-Loaded Open Dielectric Waveguides.

Jose Luis Gómez-Tornero, David Cañete Rebenaque, and Alejandro Álvarez-Melcón, *Member IEEE*

Information and Communications Department
Technical University of Cartagena
Antiguo Hospital de Marina. 30202 Cartagena, Murcia (Spain)
E-mails: josel.gomez@upct.es, david.canete@upct.es, alejandro.alvarez@upct.es
Telephone numbers: +0034 968 326531, +0034 968 325315, +0034 968 338865
Fax number: Fax:+0034 968 325973

ABSTRACT

A software tool is presented to help in the teaching of the electromagnetic theory of open dielectric waveguides. The study of the modal spectrum of canonical closed waveguides is a basic topic in any course of Electromagnetics or Microwave Engineering. However, surface-wave modes and leaky-wave modes in open waveguides are yet not so well-known in the academic environment. Nevertheless, this study is necessary, since novel open dielectric waveguides have been proposed for millimeter-waveband and optical electronics in order to reduce the conductor losses. Therefore, the comprehension of leaky-wave modes phenomenon and behavior is indispensable for any future Microwave Engineer, which will have to work with the new millimeter waveband and optical technologies. This program constitutes the first tool explicitly conceived to help the teaching of the working principles of open dielectric guides loaded with printed circuits, and the associated practical leaky-wave antennas (LWAs). The code can be a very good supplement to understand how practical LWAs work, after a basic theoretical understanding of leaky-waves has been first obtained. From the appearance of leaky-wave modes in open waveguides, to the design of a backward-to-forward leaky-wave antenna, some simple and very clarifying step-by-step exercises are presented to illustrate these not so well-known concepts. Although the program refers to a specific type of open dielectric guides (laterally-shielded, top-open, stub-loaded, rectangular dielectric waveguides with planar perturbations), the results are applicable to any open dielectric guide, helping to teach the basic theory and topics relating leaky- and surface-wave modes in uniform and periodical structures.

Keywords: Dielectric loaded waveguides, Nonhomogeneously loaded waveguides, Nonradiative dielectric waveguides, Printed circuits, Waveguide antennas, Leaky waves, Leaky wave antennas, Computer Aided Teaching.

I. INTRODUCTION

In any course of Electromagnetics, the topic of waveguides is one of the basic chapters. Rectangular, circular and coaxial waveguides can be analytically studied due to their canonical geometries, and their constitutive equations can be easily derived from Maxwell's equations [1-2]. From these equations, the set of permitted modes for each waveguide is obtained, arising to its modal spectrum. Many important and basic aspects, like the cut-off frequency, the field pattern inside the waveguide and the frequency dispersion of each mode, need to be taught to an Electric Engineer in order to understand the working principles of waveguiding. More complicated waveguides, many of them having open boundaries and planar metallizations, have been proposed for millimeter-waveband and optical electronics in order to reduce the conductor losses, while maintaining a simple geometry [3]. These novel waveguides cannot be analytically analyzed, and numerical techniques must be developed for their study [3]. Radiation from these open waveguides can occur, being an unwanted phenomenon since it creates crosstalk and radiation losses [4-5]. Moreover, radiation from open waveguides has been extensively used in order to create novel leaky-wave antennas for the millimeter waveband [6]. In any case, it is necessary to understand which conditions make a given mode of an open waveguide to radiate. Leaky-wave modes are part of the modal spectrum of open waveguides, and they can solely describe the radiated field pattern of a leaky-wave antenna under some conditions (basically, when direct radiation from the source of the open waveguide –continuous spectrum- is avoided). Therefore, the propagation and radiation characteristics of a given leaky-wave mode (maximum radiation direction, beamwidth, polarization, frequency bandwidth…) must be known and controlled to design a leaky-wave antenna (LWA). There are basically two types of LWA which provide radiation from open waveguides introducing perturbations, namely uniform and periodic LWA [6]. Figure 1 shows two uniformly loaded dielectric waveguides and one periodically perturbed guide (Fig.1-a corresponds to a uniform slitted structure, Fig.1-b is a uniform strip-loaded guide, and Fig.1-c shows a periodic strip-loaded guide). The radiation mechanisms in each type of structure (uniform or periodical) have some points in common and some differences.

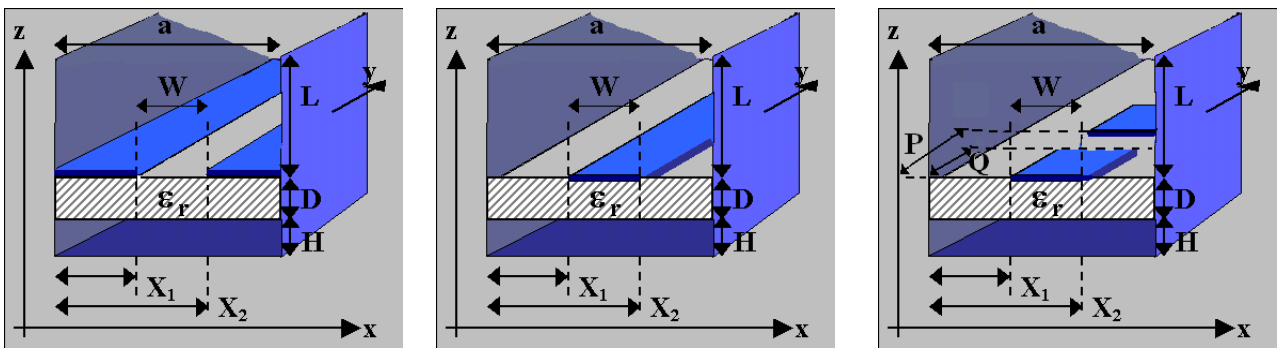

Fig. 1. Laterally-shielded open dielectric waveguides with planar perturbations.

This paper describes some simple and illustrative exercises which can be done with the help of a software tool and associated Graphical User Interface (GUI) environment, in order to understand the theory behind the propagation and radiation of leaky-waves in such laterally-shielded open dielectric guides, perturbed with planar circuitry. Leaky-wave modes have been known for the last four decades [7-8], and many articles and works have been published, studying their behavior in different open waveguides and their utility to conceive novel LWA [9-10]. The impact in the last two decades of planar technology and new open dielectric waveguides for the millimeter and optical ranges confer a more practical and urgent need to teach the future engineers the basic concepts concerning leaky-wave modes and their applications [11]. However, their study has not been introduced in the Electromagnetism education for the future Microwave Engineers yet, probably due to the absence of any commercial software capable of analyzing them in a student-friendly way. For this purpose, a novel interactive environment has been created for the analysis of leaky-wave modes in some types of laterally-shielded open waveguides, like those shown in Fig. 1. The program has been named P.A.M.E.L.A. (Program for the Modal Analysis of Laterally Shielded Structures, in Spanish), and it has been developed using MATLAB™ v.6.5, in order to take advantage of its graphical facilities. Due to the high analytical and matricial nature of the implemented method [12-13], the computations are fast enough to permit an interactive work, obtaining visual results in real time.

The main objective of this paper is to show how this program can help to teach some advanced concepts relating the nature of radiation from dielectric open waveguides loaded with uniform and periodic printed circuits. After the students have become familiar with the basic concepts of leaky waves on structures which can be studied theoretically (for instance simple dielectric layers), this code can be a good supplement to numerically analyze a more complicated (but also more practical) type of LWA structure. The GUI associated to the software is described in Section II, while the next sections present some simple but very illustrative exercises to understand the leakage phenomenon in the proposed structures. Section III presents the study of a completely shielded strip-loaded uniform dielectric waveguide. This first exercise helps to understand the working mechanism of the program, and also to easier understand what happens to the modes of a closed waveguide when it is opened. Section IV extends in the study of surface and leaky-wave modes in open dielectric guides, while the frequency response of leaky-wave modes and the transition to surface-waves is studied in detail in section V. Section VI shows how some types of leaky-wave modes can be used to conceive leaky-wave antennas (LWA). The beam direction frequency-scanning capability of LWA and the problem of the variation of the beamwidth with the frequency are also studied in this section. Section VII presents the study of a periodic structure, introducing the Space Harmonics theory and the phenomenon of backward leaky-wave radiation. Finally, section VIII shows how to use this program to analyze and design a practical backward to forward LWA. The conclusion section summarizes all the concepts that are trained using this program. These concepts can be learned by the student thanks to the combination of the mathematical expressions and the graphical results presented in this paper.

II. PROGRAM DESCRIPTION

A GUI (Graphical User Interface) has been developed to combine in a single software tool all the elements needed to obtain the modal spectrum of laterally-shielded open waveguides like those shown in Fig. 1. The main window of the program is shown in Fig. 3. The basic theory underlying the study of closed waveguides [2] must be well-known to the student. The first purpose is to obtain the propagation constants in the longitudinal direction of the waveguide (k_y, according to the reference axes of Fig. 1) for the permitted modes. For the case of leaky-wave modes, the propagation constant is complex, with a real part which is the longitudinal phase constant (β_y) and an imaginary part, also called the attenuation constant (α_y):

$$k_y = \beta_y - j\alpha_y = k_0\sqrt{\varepsilon_{reff}} \quad (m^{-1}) \tag{1}$$

where k_0 is the free-space wavenumber and ε_{reff} is the effective relative constant, which can have in general a complex value. The complex nature of the longitudinal propagation constant is due to the decrease of the amplitude of the leaky-wave mode as it propagates through the open waveguide, as it can be inferred from the inverse Fourier transform of a sinusoidal time varying field:

$$\tilde{A}(k_y) = e^{-jk_y\cdot y} = e^{-j(\beta_y - j\alpha_y)\cdot y} = e^{-j\beta_y\cdot y}\cdot e^{-\alpha_y\cdot y} \tag{2}$$

$$A(\omega_0 t) = \Re e\left\{\tilde{A}(k_y)\cdot e^{j\omega_0 t}\right\} = e^{-\alpha_y\cdot y}\cdot\cos\left(\omega_0 t - \beta_y\cdot y\right) \tag{3}$$

This attenuation might be caused by radiation losses, that is, the mode suffers leakage of power as it propagates, radiating at a given angle θ_m, and it is therefore called a leaky-wave mode. Figure 2 illustrates this phenomenon.

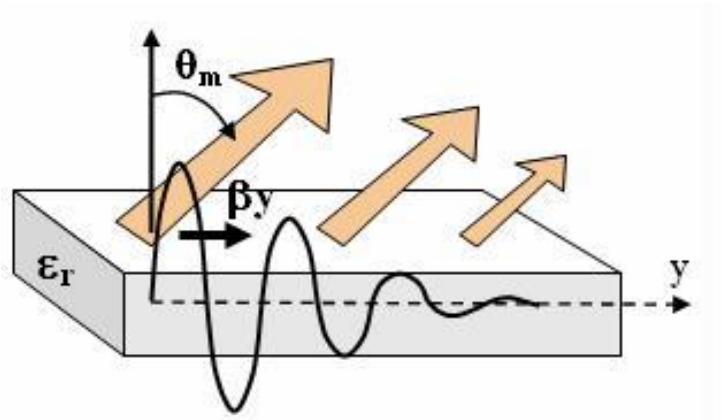

Fig. 2. Leaky-wave mode propagating and radiating from a dielectric guide.

Figure 3 shows the main window of PAMELA, a program specifically developed to study and teach leaky-wave modes in a visual and interactive way.

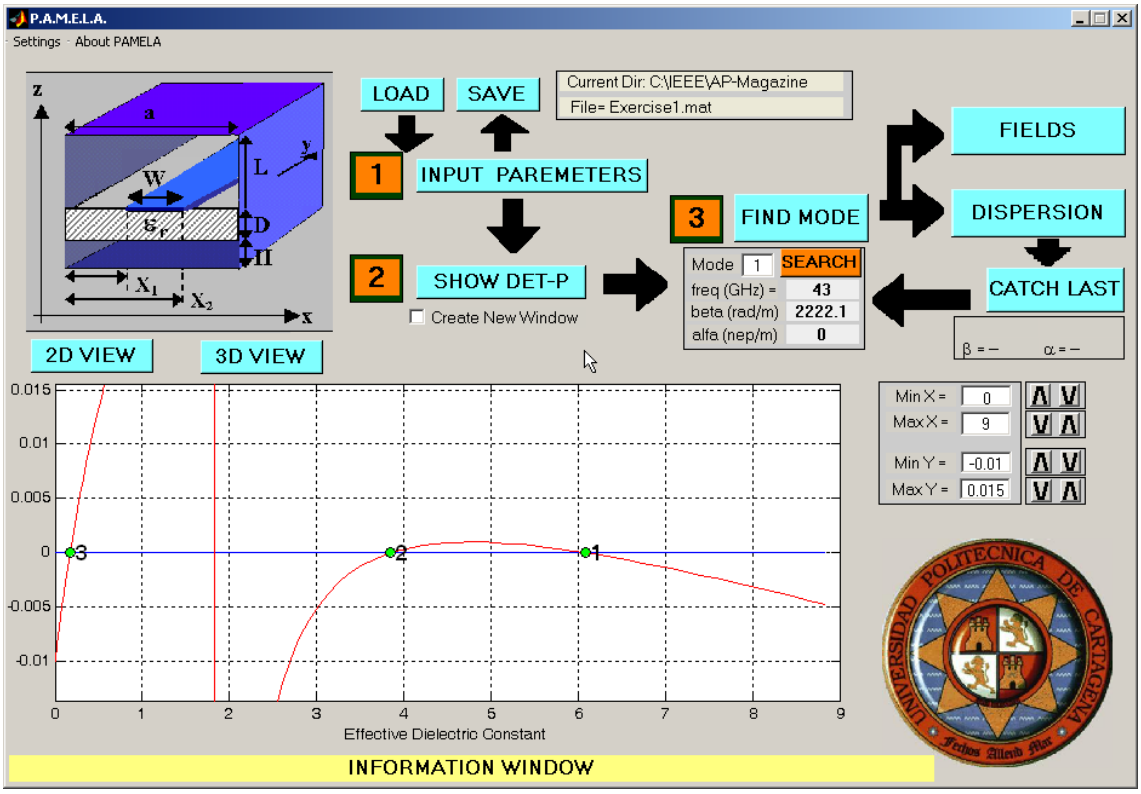

Fig. 3. Main Window of P.A.M.E.L.A. Graphical User Interface.

The user must first choose the type of structure to be studied (strip, slot, no planar metallization…) and introduce the values for its geometrical parameters (according to Fig.1) using the Input Parameter window, which appears when the button indicated with the number *1* (*Input Parameter*s) in Fig.3 is pressed. The top-left region of the main window shows a figure of the type of structure which is being analyzed (strip/slot, closed/open waveguide, uniform/periodical…), together with its constitutive dimensions, as shown in Fig.1. Load and save controls permit to store in a text file the parameters introduced in the main window (geometrical parameters of the structure and numerical parameters for the analysis), and allow to recover them in a new session. The numerical method used for the electromagnetic analysis is based on the Method of Moments (MoM), and the formulation can be found in [12-13]. The kernel of the program computes the determinant of the MoM matrix (*detP*). This determinant is a function which depends on the geometry, the frequency and the value of k_y. A given k_y value will be a solution of Maxwell's equations for a given geometry *G* and frequency *f*, if the following condition is satisfied:

$$\det P = \Phi(G, f, k_y) = 0 \tag{4}$$

Using the Input Parameter window (button *1* of Fig.3*)*, the user must also introduce the parameters for the computation of Φ: frequency of analysis, *f*, and the range of values ε_{reff} for which the function $\Phi(k_y)$ will be *computed in the real* β_y *axis*. In this way, by pressing the Show Det-P button (number *2* in Fig.3), the

function $\Phi(k_y)$ will be computed and the results plotted at the window shown at the bottom of Fig. 3. A given solution (a mode of the waveguide) of the analyzed waveguide exists each time this graph crosses the zero level. Using the *Find Mode* button (number *3* in Fig. 3), the user can find the chosen zero of $\Phi(k_y)$, which corresponds to a permitted mode. As it will be explained throughout this paper, two different types of modes can be searched, namely closed waveguide modes and open waveguide modes, which can be selected using the controls associated to the *Find Mode* button. For instance, Fig. 3 shows that the program has found 3 modes in a microstrip closed waveguide. Once a given k_y solution has been found, its fields (currents, electric field, magnetic field, power density, radiation pattern) can be plotted in 1D or 2D using the controls associated to the button *Fields* shown in Fig. 3. The fields distribution will be plotted in new windows, which can be saved or printed. Besides, the solution found can be used to make a dispersion analysis, which can be done using the frequency as the sweep parameter, or by sweeping any geometrical parameter of the structure. The button labeled *Dispersion* in Fig. 3 is used for this purpose. Figure 4 shows the block functional diagram of the program. In the next sections, some examples will illustrate the working principle of this program, and the type of results which can be obtained to teach the leaky-wave phenomenon and its applications.

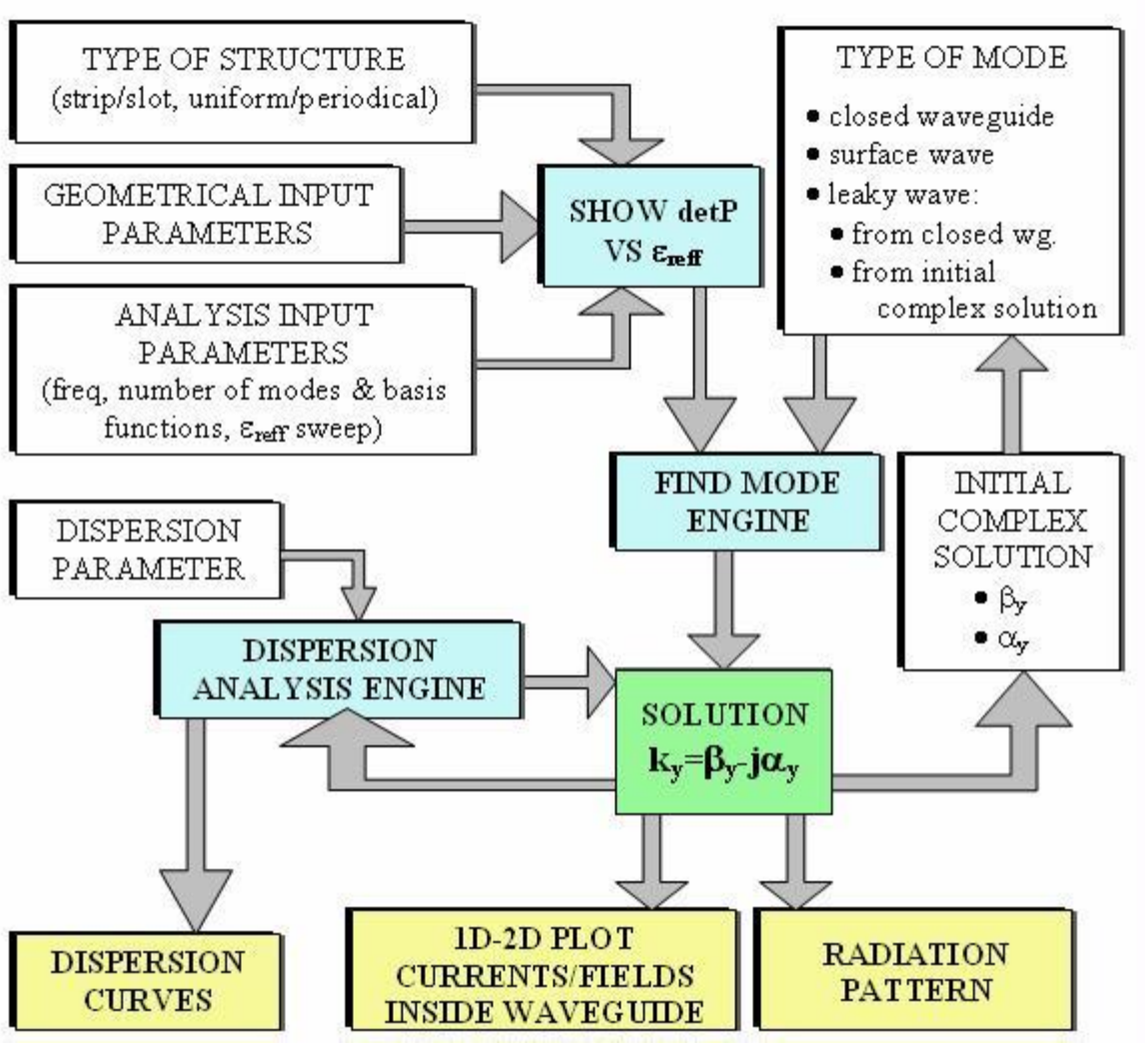

Fig. 4. Diagram of Functional Blocks of P.A.M.E.L.A.

III. REAL MODES IN CLOSED WAVEGUIDES

To easier understand the theory involved in the propagation of modes in open waveguides, it is better to start by studying the corresponding completely shielded waveguide, and later proceed by opening it. To illustrate it, a uniform strip-loaded dielectric waveguide (as that shown in Fig.1-b) is going to be analyzed now. The user must choose a strip-type structure and insert the value for each geometrical parameter, using the *Input Parameter* window shown in Fig.5 , which is associated to button 1 of the main window (Fig.3). Figure 5 also shows the dimensions of the proposed structure for this first exercise.

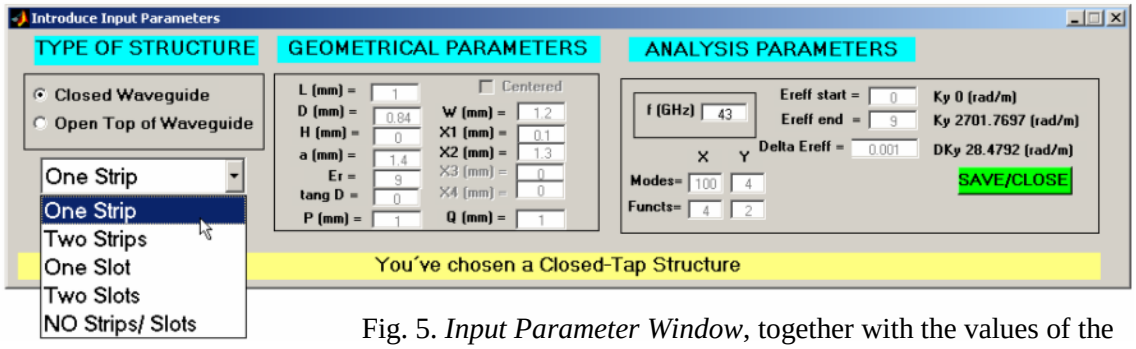

Fig. 5. *Input Parameter Window*, together with the values of the geometrical and analytical parameters for the first exercise.

The proposed completely-closed dielectric guide has a relative dielectric permittivity $\varepsilon_r=9$, with a strip of width $W=X_2-X_1=1.2mm$ located symmetrically with respect to the lateral metal walls, which are separated at a distance $a=1.4mm$ ($X_1=0.1mm$, $X_2=1.3mm$). As commented, the kernel of the program computes the determinant of a matrix obtained by a numerical procedure (Method of Moments), which is obtained for a range of values of the effective relative dielectric constant $\varepsilon reff$, related to the longitudinal propagation constant k_y by Eq.(1). ε_{reff} is going to be swept from $\varepsilon_{reff}=0$ to $\varepsilon_{reff}=9$, which is the range of all possible real positive values for ε_{reff} , since the dielectric substrate used has $\varepsilon_r=9$. The analysis is performed at a fixed frequency of $f=43GHz$. The user must press button 2 of the main window in Fig.3, *Show Det-P*, and the program calculates the function $detP=\Phi(k_y)=\Phi(\varepsilon_{reff})$ and then plots a graph with the real and the imaginary parts of the determinant at the bottom of the main window, as shown in Fig.3. A detail of this graph is presented in Fig.6, where it can also be seen that there are three different solutions at this frequency of 43GHz. Each one corresponds to a zero of the function $\Phi(k_y)$, and therefore to a permitted mode of the closed waveguide. These modes are said to be **real modes**, since they have a real k_y solution.

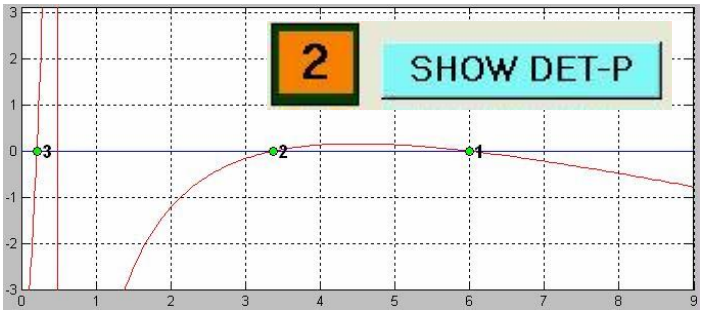

Fig. 6. Computation and plot of the determinant of the MoM matrix (detP), for the closed waveguide loaded with a symmetrically located strip. Three different real modes are observed at the frequency of 43GHz.

To find a given mode, the user must press the *Find Mode* button, which corresponds to step 3 of the main window in Fig.3. A new dialog window appears, in which the type of mode to be searched must be selected (Fig.7). In this first example, we are interested in the study of real modes, since the structure is completely closed. The user must also choose the order of the mode to be found, being the first mode the dominant one, that is, the one which appears at a higher value of ε_{reff} in the *detP* graph. Figure 7 shows the dialog windows to find the first mode. Once the user presses the *Search* button of this window, a circle with the order of the mode found appears in the position of the corresponding zero of the *detP* graph (see Fig.6). The values of β_y and α_y of the propagation constant of the chosen mode come into view below the *Find Mode* button, together with the frequency of analysis, as shown in Fig.7.

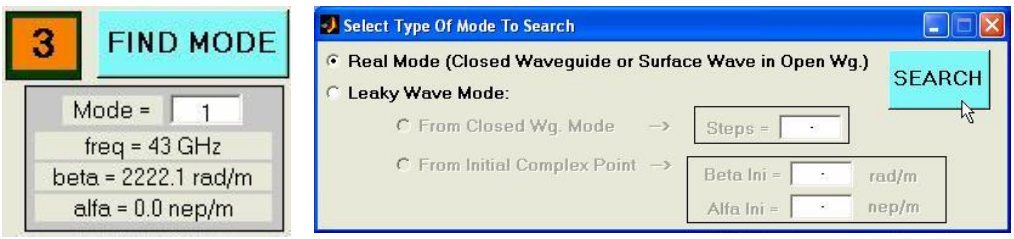

Fig. 7. *Find Mode* dialog window, showing the values of the first real mode in the closed waveguide.

Once a given mode has been found, different types of plots of the electric, magnetic, current and power density fields can be obtained using the button *Fields* (Fig.3), which opens the dialog window shown in Fig.8. This figure shows how to plot the Electric fields in the cross section of the closed waveguide (y=0 plane, transverse Z-X coordinates). This window also allows to determine the resolution of the grid used to plot the fields.

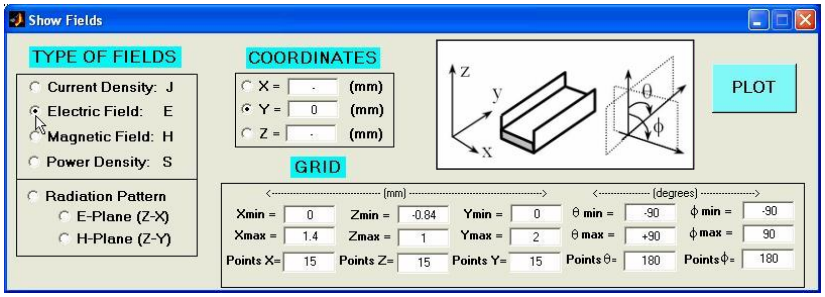

Fig. 8. *Show Fields* dialog window, showing the controls to plot the electromagnetic fields of the mode found in the previous step.

By pressing the *Plot* button, new windows appear with the different components of the vector fields. The representation of the fields informs about the nature of each mode, and helps the student to understand in a more visual way the structural differences of each type of mode [11], as it will be illustrated. Figure 9 shows the transverse components (x and z directed) of the electric field in the cross section of the waveguide (plane y=0) for the three real modes found in the closed strip loaded structure.

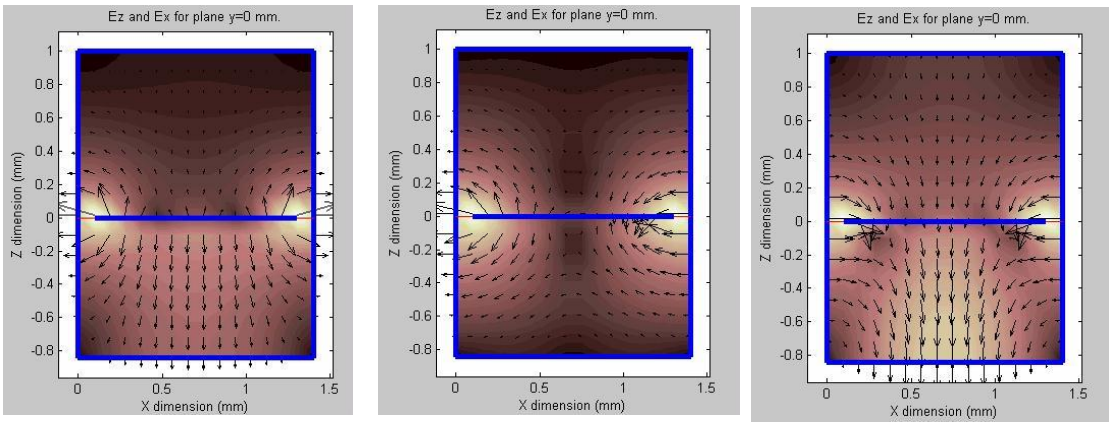

Mode 1
Quasi Static

Mode 2
Channel Guide

Mode 3
Perturbed TE_{10}

Fig. 9. Transverse components of the Electric Field of the three real modes in the closed structure.

The dominant mode (mode 1), corresponds to the quasi-static solution of the two-conductor structure, that is, a mode whose electric field is directed from the strip conductor to the rectangular shield walls (if the shield was less closed to the strip, and the dielectric thickness *D* was lowered, this mode would be the so well-known main mode of a microstrip line.) The second mode is called a channel-guide mode [14], since the electric field lines emerge from one of the lateral metallic walls and goes to the opposite side, as if it was guided between the channel waveguide formed by the two parallel-plates. However, this horizontal electric field is perturbed by the strip, which makes the field lines to couple to it as it can be seen in Fig.9. The third and last mode is basically the TE_{10} mode of the rectangular dielectric guide, but perturbed by the two slots created at both sides of the centered strip. It can be seen from Fig.9 that the net electric field polarization is vertical, in opposition to the net horizontal field of the channel guide mode. It is important to notice this difference to understand their utility for leaky-wave antennas.

IV. OPEN WAVEGUIDES: LEAKY-WAVE MODES AND SURFACE-WAVE MODES

The strip-loaded dielectric guide is opened in its top side by selecting "*Open Top of Waveguide*" in the *Input Parameter* window (Fig.5). The user must plot the new $\Phi(\varepsilon_{reff})$ function using the *Show Det-P* button, as previously done, obtaining the result shown in Fig.10.

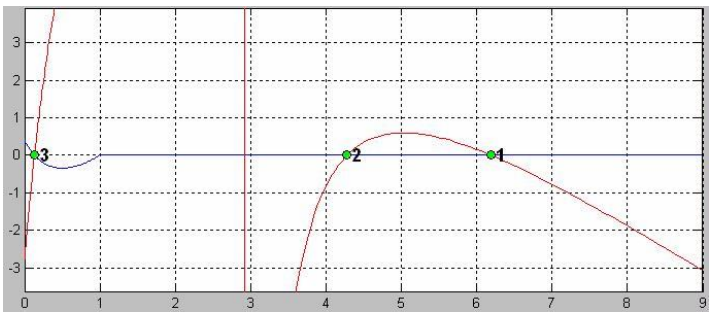

Fig. 10. Plot of detP, for the open waveguide loaded with a symmetrically located strip (*f=43GHz*).

The graph seems to be essentially similar to that obtained in Fig.6, observing again three different possible modes in the structure. It looks as if the open waveguide behaves the same as the closed waveguide. However, the student must realize that something very important has happened to the *detP* for values of ε_{reff} below $\varepsilon_{reff}=1$. The real part of detP, which was equal to zero for all the range of variation of ε_{reff} in the closed waveguide case (see Fig.6), differs now from zero below $\varepsilon_{reff}=1$. However, the third zero of detP subsists because both the real and the imaginary part of *detP* becomes zero at a given *εreff* solution below $\varepsilon_{reff}=1$, producing the mode number 3. To understand the radiation mechanism, the user must change the position of the strip, which now must be ***located asymmetrically*** with respect to the lateral walls and ***attached to one of the side*** walls ($X_1=0mm$, $X_2=1.1mm$). The new graph of detP for this asymmetrically loaded open waveguide is shown in Fig.11.

Fig. 11. Plot of detP, for the open waveguide loaded with an asymmetrically located strip, attached to a side wall (*f=43GHz*).

Two main differences are observed in the new plot, with respect to the symmetrically located strip (Fig.10). First of all, it can be seen only one mode above $\varepsilon_{reff}=1$, which corresponds to the Channel Guide mode of the closed structure (mode 2 in Figs.6, 9 and 10). The fundamental mode of the closed structure (the quasi static mode) has disappeared due to the fact that now there is only one conductor in the waveguide (the strip is short circuited to the side wall). Therefore, the quasi static solution (which is originated by a potential difference between two different conductors) cannot exist. Second, the third mode of Figs.6 and 10 (perturbed TE_{10} mode in Fig.9), which was below the $\varepsilon_{reff}=1$ limit, has also disappeared. In the asymmetric structure, the real and imaginary parts of detP are both different from zero for $\varepsilon_{reff}<1$. This last condition is of much importance, since the solution might not be anymore in the real k_y axis, but it can migrate to the complex k_y plane. To perform a search of a given complex mode, the user must select in the *Find Mode* window the *Leaky-Wave mode* search option, as shown in Fig.12. This search can be done in two different ways. The user can introduce the coordinates in the complex plane of a given Initial Point (β_y and α_y), which must be an initial guess, from which the program will search for a zero of $detP(k_y)$. Should the initial guess be close to the final solution of the open waveguide, it is more probable for the program to succeed in the search of the complex solution. Another way consists in the use of the real solution of the closed waveguide as the initial guess to search for the complex mode of the open waveguide. An original iterative algorithm has been implemented [15], in which the top boundary conditions are changed from that of a metal wall (closed waveguide) to that of an open waveguide. If this change is made in small steps, the program can track the variation of the solution from the real β_y axis to the complex $k_y=\beta_y-j\alpha_y$ plane. For this purpose, the

user must introduce the order of the real mode of the closed waveguide to be used as initial point (see the *Mode* input box under button 3 in Fig.3), and the number of steps in which the aforementioned iterative search must be executed (see the *Steps* input box in Fig,12). Figure 12-a shows the results obtained for the search of the complex mode by starting from the second mode of the closed *asymmetric* waveguide. Remember that the quasi static mode has disappeared due to the connection of the strip to a lateral wall of the box. In this case, the first mode is the channel-guide mode and the studied perturbed TE_{10} mode becomes the second mode. A new window is opened showing the step-by-step movement in the complex k_y plane, so the student can see how the real mode moves into the complex k_y plane as the top wall is open. The final value of this leaky-wave mode complex propagation constant at *43GHz* is $k_y=747.24-j12.85$ (m^{-1}). Also this movement is added in the *Show DetP* graph of the main window.

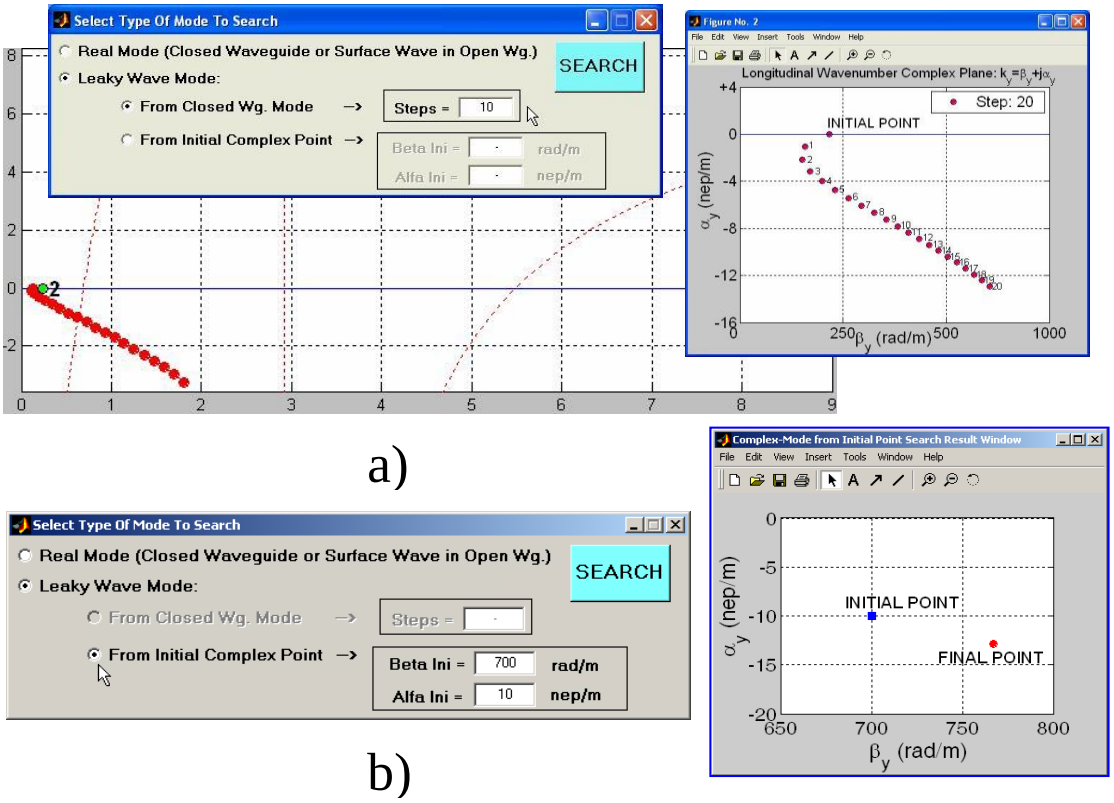

Fig. 12. a) Iterative search of leaky-wave mode in the asymmetrical open waveguide by starting from the corresponding real mode of the closed waveguide (*f=43GHz*) b) Search using an initial guess of the solution.

The user can also introduce an initial guess for the complex k_y solution to be used as a starting point in the search algorithm, as shown in Fig.12-b (where the point $k_y=700-j10$ was used as initial point). The questions that must be made at this point are the next: Why is the Channel Guide mode a real mode independently on the waveguide top cover (closed or open)? And, why has the perturbed TE_{10} mode moved to the complex plane in the case of the asymmetrical open structure, while it is a real mode for the case of the centered strip open waveguide? To answer these questions, a little bit of mathematics is needed. The z-directed propagation constant in the vacuum medium for a plane wave can be written using the next expression:

$$k_z = \sqrt{k_0^2 - k_x^2 - k_y^2} \tag{5}$$

being k_y the longitudinal propagation constant of a given mode in the studied open waveguide. Any of the studied modes is determined by a k_y value. However, the fields variation in the transverse direction cannot be modeled by a simple plane-wave variation. The variation of the field of any mode in the transverse direction is more complicated. Nevertheless, any mode of the laterally-shielded waveguide can be expressed as a contribution of the orthogonal set of parallel-plate modes (PPM) supported by the lateral walls (separated at a distance a). In this way, it can be said that each mode of the open waveguide is created by the convergent summation of many PPM, each one characterized by its harmonic variation in the x-direction:

$$k_{xm} = m\frac{\pi}{a} \tag{6}$$

In the case that the main PPM ($m=0 \rightarrow k_{xm}=0$) is excited in a given waveguide mode, Eq.(5) can be used to determine its z-propagation constant in the vacuum, obtaining the next result:

$$k_{z,m=0} = \sqrt{k_0^2 - k_y^2} \tag{7}$$

This transverse propagation constant must be real to allow this main PPM to radiate, that is, to be above cut-off in the vacuum medium. Therefore, the radiation condition for the main PPM can be written as follows:

$$\text{Radiation Region} \rightarrow \quad k_0 > k_y \quad \rightarrow \quad \frac{k_y}{k_0} = \sqrt{\varepsilon_{reff}} < 1 \tag{8}$$

Therefore, it can be said that $\varepsilon_{reff}=1$ is the limit of the radiation region for the main PPM. For higher-order PPM, this condition is more restrictive, that is, k_y must have a still lower value (which can be easily obtained by introducing Eq.(6) into Eq.(5)). Since any mode of the laterally-shielded open waveguide can be expressed as a summation of PPM, it is necessary that at least one of these PPM radiates in order to say that the waveguide is radiating. For this reason, it can be said that above $\varepsilon_{reff}=1$ ($k_y/k_0=1$), none of the modes of the open waveguide can radiate, since all the energy is below cut-off in the vacuum. In this case, it is said that the mode is a ***surface-wave mode***, having a real k_y (and ε_{reff}), which means that all its propagating energy is confined in the dielectric slab. This is the case of the Channel Guide mode shown in Fig.11, whose ε_{reff} is real and above unity. The radiation region ($k_y/k_0<1$) is also called ***"fast-wave" region***, since the mode has a longitudinal phase velocity greater than the velocity of light in vacuum [16].

However, the second question is not answered yet. Figure 10 showed a real solution (TE_{10} mode) below the $\varepsilon_{reff}=1$ limit for the symmetrically located strip, while for the asymmetry case (Fig.11) this mode became a complex mode. To understand this phenomenon, the student must obtain the electric field pattern inside the waveguide for these two cases, shown in Fig.13-a and –b.

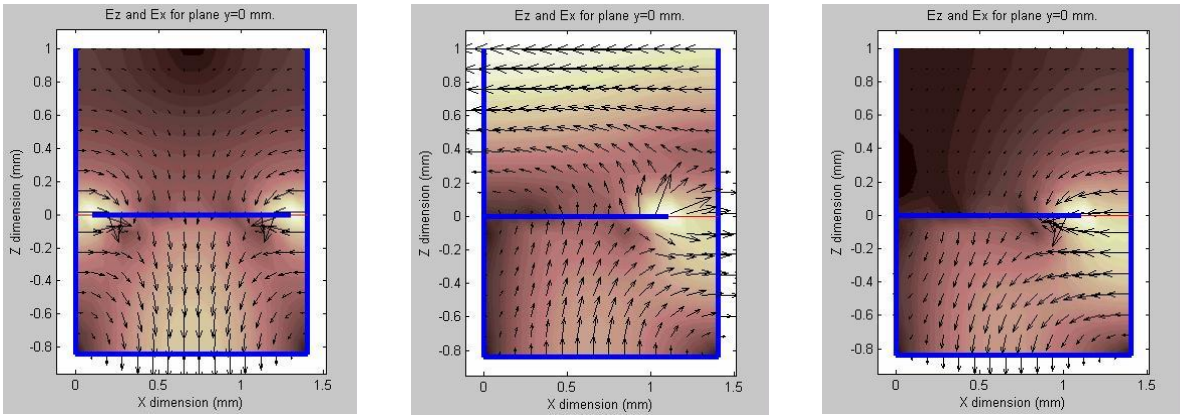

a) b) c)

Fig. 13. Transverse electric field patterns inside open waveguide for different scenarios:
a) Symmetrically perturbed TE_{10} mode @43GHz → Surface Wave
b) Asymmetrically perturbed TE_{10} mode @43GHz → Leaky Wave
c) Asymmetrically perturbed TE_{10} mode @60GHz → Surface Wave

For the case of the symmetrically perturbed TE_{10} mode, the main PPM (*m=0*) is not excited, therefore not leading to a net radiation. As can be seen fromFig.13-a, all the energy is confined in the dielectric guide region (bottom of the guide), while in the top air-filled region the field is evanescent. On the contrary, for the asymmetrically located strip, the main PPM (*m=0*) is excited and radiation occurs (remember that *m=0* can propagate in the vacuum region). This main PPM has no variation in the x-direction ($k_{xm}=0$), which means that the electric field has a horizontal transverse electric field, going from one of the side walls to the other with a constant amplitude. This constant horizontal field component can only be excited by the TE_{10} mode if the perturbation is located asymmetrically, inducing a difference of potential between the two side walls. All these phenomena are clearly shown in Fig.13-a and Fig.13-b.

At this point, the student must have acquired the next conclusions relating the change from the modal spectrum of the closed symmetrical waveguide to the open asymmetrical waveguide:

1) The attachment of the strip to the side of the waveguide makes the quasi static mode to disappear from the modal spectrum of the waveguide (closed or open).
2) The radiation region of any mode is the so called "*fast-wave*" region, in which the ε_{reff} value is below unity.
3) To make the mode radiate (leaky-wave mode), the main parallel-plate mode ($k_{x,m=0}=0$) of the laterally shielded waveguide must be excited, since this mode is the only above cut-off in the air region, and therefore responsible for the radiation mechanism.
4) The TE_{10} mode of the rectangular dielectric guide must be perturbed asymmetrically to make it radiate, since the asymmetry is responsible of the excitation of the main parallel-plate mode (*m=0*). If the planar perturbation (strip or slot) is located symmetrically with respect to the side walls, the mode is a surface-wave mode even in its "*fast-wave*" region, since the main PPM (*m=0*) is not excited.

V. FREQUENCY DISPERSION. RADIATION FROM LEAKY-WAVE MODES.

All previous results have been obtained for a fixed frequency value (*43GHz*). The frequency dispersion of the leaky-wave modes must be studied to understand the behavior of the open waveguide for different frequencies. Once a given mode has been found at a fixed frequency, a dispersion analysis can be performed using the P.A.M.E.L.A. environment. The user must press the *Dispersion* button of the main window, and a new *Dispersion Analysis* window (see Fig.14) will open. The user must select which parameter to sweep (in our case it is the frequency), the range of variation (in our case, from *43GHz* to *100GHz*) and the type of figures to plot (k_y in the complex plane, β_y, α_y and/or radiation angles –beam direction θ_m and beamwidth $\Delta\theta$). By pressing the *Compute* button, the program will start to make the simulations and will plot the results.

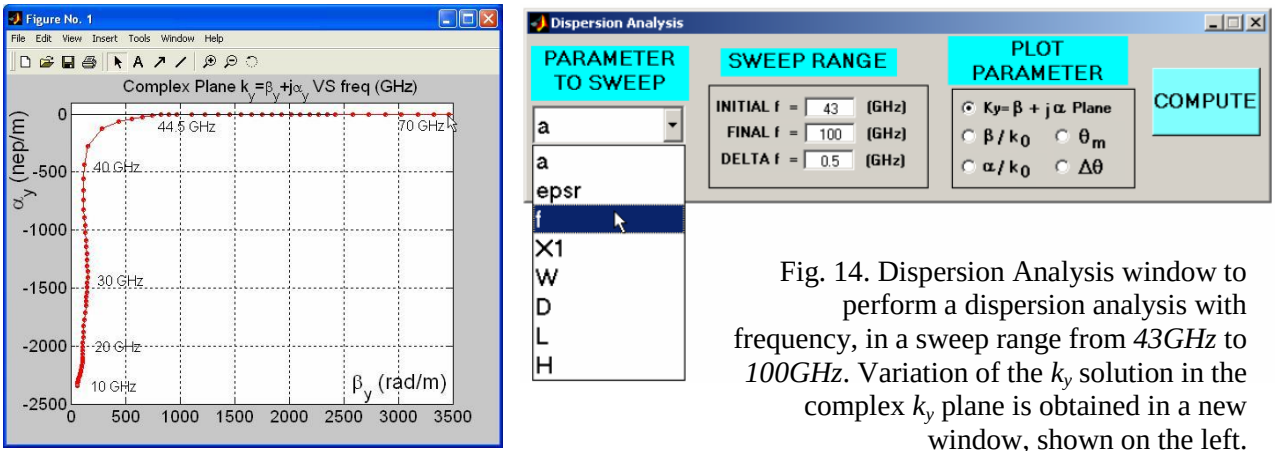

Fig. 14. Dispersion Analysis window to perform a dispersion analysis with frequency, in a sweep range from *43GHz* to *100GHz*. Variation of the k_y solution in the complex k_y plane is obtained in a new window, shown on the left.

Figure 14 shows the results window obtained to see the variation of the ky solution in the complex plane, for the perturbed TE_{10} leaky-wave mode, as the frequency is varied from *10GHz* to *100GHz*. It can be seen that the solution becomes real ($k_y=\beta_y$, $\alpha_y=0$) for frequencies above *44.5GHz*. This phenomenon is called leaky-to-surface wave transition, and occurs in all open dielectric waveguides [16]. By observing separately the evolution of the real and the imaginary parts of k_y, and expressing them normalized with respect to k_0, new and interesting conclusions can be obtained.

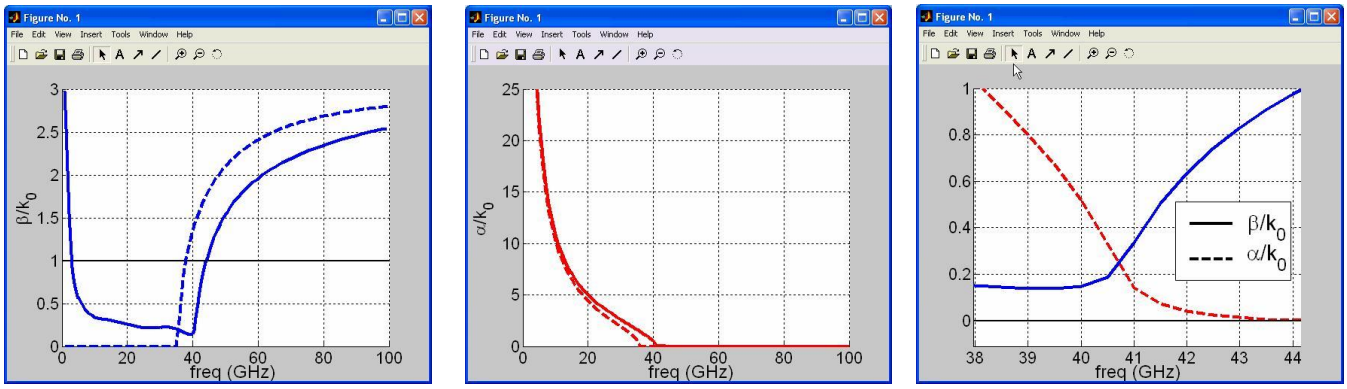

a) b) c)

Fig. 15. Dispersion of normalized phase and attenuation constants with frequency.

Figure 15-a shows the dispersion with frequency (*0-100GHz*) of the normalized phase constant for the perturbed TE_{10} leaky-mode (β_y/k_0). The student is asked to compute the well-known frequency dispersion of the TE_{10} mode of the completely closed rectangular dielectric guide used in this structure (width *a=1.4mm*, height *D=0.84mm*, substrate $\varepsilon r=9$) and plot it together with the perturbed TE_{10} mode obtained with the program. The TE_{10} mode curve is plotted in Fig.15-a with dashed line, while the perturbed TE_{10} mode is represented in continuous line. In this way, the student can see how both dispersion curves behave in a similar way, having the perturbed mode a lower phase constant due to the fact that the field propagates in an inhomogeneous medium, between the dielectric slab and the air region. However, an important difference is seen in Fig.15-a. When the real TE_{10} mode reaches its cut-off zone (below *35GHz*) the phase constant becomes zero, since the propagation constant becomes purely real. However, for a leaky-wave mode, the normalized phase constant reaches a stable value different from zero below a given frequency, which seems to be related to the cut-off region.

Figure 15-b shows the variation of the attenuation constant for both the analytical TE_{10} mode of the dielectric rectangular closed guide (dashed line), and the perturbed leaky-wave TE_{10} mode of the open waveguide (continuous line). Again, these two plots are quite similar, observing a rapid increase of α/k_0 as the frequency decreases in the cut-off region. However, the cut-off region and the radiation region of a leaky-wave mode must not be confused. For this purpose, Fig.15-c shows a detailed plot of β/k_0 and α/k_0 for the perturbed TE_{10} leaky-wave mode. Above *44.5GHz*, α_y/k_0 becomes zero, which is due to the conversion of the mode to a surface-wave, therefore eliminating the radiation phenomenon. Below this transition frequency, α_y/k_0 rises in a smooth way. This region is the radiation region, whose upper limit was established by Eq.(8). Moreover, below *41GHz*, the attenuation constant increases in a rapid way, following the typical curve of the imaginary part of a TE_{10} mode below cut-off in a standard waveguide (see Fig.15-b). The attenuation constant α_y can be divided into two different parts, namely the reactive attenuation constant and the radiative attenuation constant:

$$\alpha_y = \alpha_y^{RAD} + \alpha_y^{REACT} \tag{9}$$

Both parts contribute to the decreasing amplitude behavior of the mode as it propagates along the waveguide axis. However, the reactive attenuation corresponds to the mode carrying reactive power (mode below cut-off), while the radiative attenuation part accounts for the radiation losses (energy radiated to space). In the cut-off region, α^{REACT} dominates the radiation losses rate. This region can also be limited by the next condition, which has been checked by numerical measurements [17]:

$$\text{Cut-off Region} \rightarrow \frac{\alpha_y}{k_0} > \frac{\beta_y}{k_0} \tag{10}$$

This last condition, together with the radiation upper limit (transition to surface-wave), allows gathering in a numerical expression the limits of the ***radiation region*** of a leaky-wave mode, once it is known the values of the phase and attenuation constants:

$$\text{Radiation Region Limits of a Leaky-Wave mode} \rightarrow \quad \frac{\alpha_y}{k_0} < \frac{\beta_y}{k_0} < 1 \tag{11}$$

These limits establish the practical frequency bandwidth of radiation of a LWA. Fig.13-c shows the electric field pattern for the perturbed TE_{10} mode at *60GHz*. At this frequency the mode has made the transition to a surface-wave; it can be seen from the plot that the energy is confined in the dielectric region, and no fields propagate through the vacuum region. The spectral-gap associated to the transition between the leaky and surface regimes [16] can also be found by PAMELA. In this region, a mode can be leaky even when it is in the slow-wave zone. However, this regime is out of the scope of the illustrative examples described in this paper. The radiation pattern of a leaky-wave mode is that of an exponentially decreasing illuminated aperture, obtaining a narrow beam radiating at a given angle θ_m, measured from the broadside direction (see Fig.2). The resulting main beam direction (θ_m) and the 3dB beamwidth ($\Delta\theta$) can be approximated by [6]:

$$\sin\theta_m \cong \frac{\beta_y}{k_0} \tag{12}$$

$$\Delta\theta \cong \frac{1}{\frac{L_A}{\lambda_0}\cos\theta_m} \approx \frac{\alpha_y / k_0}{0.183 \cdot \cos\theta_m} \tag{13}$$

These expressions are used by the program to compute the characteristics of the main radiated beam from the phase and attenuation constant of a leaky-wave mode. Figure 16 shows the results obtained from the perturbed TE_{10} mode, in its radiation bandwidth (*41-44.5GHz*). Also a plot of the transverse power density flux inside the waveguide and the numerical radiated patterns (E- and H-planes) are shown in Fig.16. It can be seen that the energy flows from the dielectric guide to the air region. The parallel-plate stub is needed to focus the energy, avoiding unwanted grating lobes and cross-polarization. It can be seen from Fig.13-b how the field emerging from the dielectric guide has a reactive zone, above which the electric field polarization becomes purely horizontal. Also in Fig.16-b it is seen that the outgoing power flux lines are focused by the parallel-plate stub once they have propagated a given height. The computed radiated pattern, observed in Fig.16-b, is that of a narrow beam tilted at an elevation angle θ_m in the H-plane (Y-Z plane), with some secondary lobes. This narrow beam in the H-plane is due to the high effective radiating surface of a LWA, obtained from the exponentially decaying illumination of the waveguide aperture. From Eq.(13) it is seen that, as the attenuation rate α_y is lower, the radiated beam is narrower, obtaining higher antenna directivities. In the E-plane (X-Z plane) a not so narrow beam, broadside directed with respect to the azimuth angle ϕ, is obtained. Array techniques can be used to increase the directivity in this E-plane.

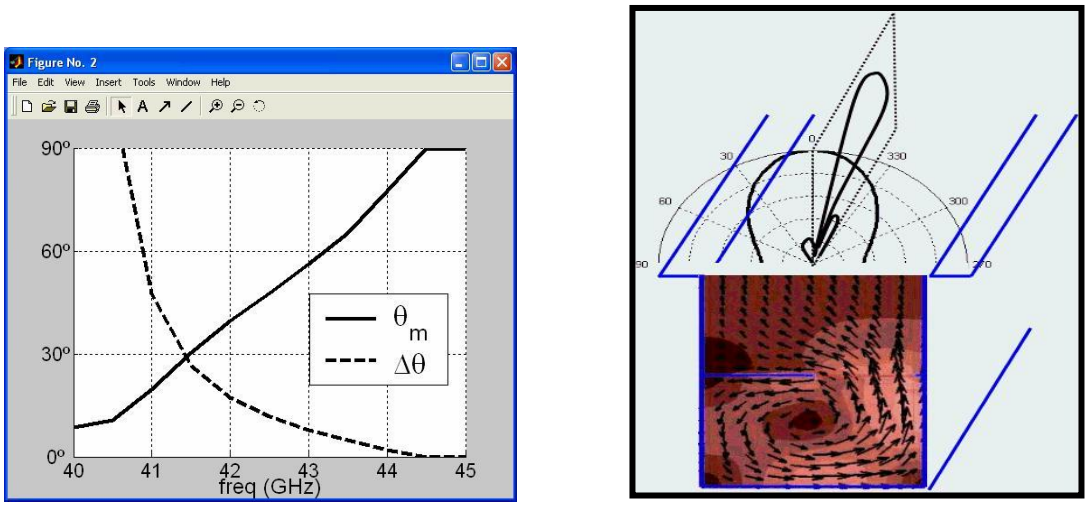

a) b)

Fig. 16. a) Variation of the beam main direction and beamwidth with frequency. b) Power density pattern inside the waveguide and radiated by the perturbed TE_{10} leaky-mode (*f=43GHz*).

Two further important conclusions about LWA can be obtained from Fig.16-a. According to Eq.(12), the angle of maximum radiation θ_m directly depends on the normalized phase constant β_y/k_0 of the leaky-mode. Since the phase constant of a leaky-wave mode (in our case, the perturbed TE_{10} mode) is clearly dispersive with the frequency, the pointing direction of a LWA is scanned with the frequency. In particular, and according to Eq.(8) and the variation of βy observed in Fig.15-c, it can be seen in Fig.16-a how this θ_m angle is scanned from near the broadside direction obtained at the lower frequency limit ($\theta_m=12^o$ at *40.5GHz*) to the endfire direction, which is reached near the transition to surface-wave ($\theta_m=90^o$ at *44.5GHz*). This is the first important feature of a leaky-wave mode; the frequency scanning-angle behavior. This can be of much interest in some applications (RADAR, tracking…), but it can also limit the bandwidth for fixed beam applications. The other interesting characteristic is related to the beamwidth frequency response. In Fig.16-a it is seen that the beamwidth $\Delta\theta$ strongly varies with the frequency, having a narrower beam as the frequency increases. In the cut-off region (below *41GHz*), the beamwidth seems to rise, due to the rapid increase of α_y due to the reactive attenuation. However, the radiated beamwidth formula has no physical meaning outside the radiation region. The variation of the beamwidth with the frequency can be an annoying effect in many applications, where the same directivity is needed for different pointing directions.

At the end of this second exercise, the student must have understood the next important topics relating leaky-wave modes behavior:

1) Leaky-wave modes in open dielectric waveguides have an effective radiation frequency bandwidth, limited by the cut-off region and the surface-wave region. The limits of these regions can be obtained from the leaky-wave mode phase and attenuation constants.
2) The attenuation constant of a leak-wave mode can be divided into two different contributions, one due to reactive attenuation and the other due to radiative losses, being the first dominant in the cut-off region.

3) LWA have large bandwidths, due to their traveling-wave nature, in opposition to the resonance radiation mechanism of other type of antennas (printed circuit patches or slots), whose bandwidth is much more limited.
4) High gains in the H-plane can be obtained from LWA by exciting a weakly attenuated leaky-wave mode. However, to enhance the low directivity in the E-plane, arrays of LWAs must be used.
5) Dielectric filled LWA present the capability to scan the pointing direction with frequency, from near broadside to endfire. The beamwidth also varies with the frequency.

VI. UNIFORM LEAKY-WAVE ANTENNA DESIGN.

Once the student is familiar to the leaky-wave phenomenon in open dielectric waveguides, we can start with the design of uniform LWA. The main idea for a versatile LWA design is to find a structure in which the leakage rate (α_y) of a given leaky-wave mode can be varied while maintaining unchanged its phase constant (β_y). This is necessary for three practical reasons:

1) According to Eq.(12-13), if one can change α_y without perturbing β_y, the beamwidth can be controlled in a wide range (from narrow to wide beams), independently of the scan angle of the antenna.
2) Moreover, the illumination of a practical LWA must be adjusted to a given pattern in order to control sidelobes [6]. For this purpose, the attenuation constant α_y is varied along the length of the antenna. However, the antenna must radiate at the same angle at any point, which means that β_y must remain constant all along the antenna length, for the different values of α_y.
3) When feeding a LWA, the source must inject power to the open waveguide. To avoid direct radiation from the source discontinuity and to obtain an optimum matching, it is desirable that the input section of the antenna does not radiate. From this non-radiative waveguide ($\alpha_y=0$), the section of the LWA must be smoothly varied to obtain the final radiation rate ($\alpha_y \neq 0$); in this variation of α_y, the phase constant of the leaky-wave mode must remain unchanged to radiate at a single angle, avoiding mismatch between the source and the antenna.

Not all the leaky-wave modes allow to control their phase and attenuation constants in such an independent fashion. Moreover, the LWA designer must find which geometrical parameter of the cross section of the antenna can be modified to vary α_y in a wide range, while not perturbing β_y. Besides, the

parameter chosen to control the radiation of the antenna must be modulated along the length of the antenna for a practical tapered design. It is of much practical interest that the modification of this parameter of the open waveguide is mechanically simple to realize. Therefore, the design of a practical and versatile LWA is not a trivial task, and many research works have been published on this topic. Using the P.A.M.E.L.A. tool, a recent and original type of hybrid planar-waveguide technology LWA design has been proposed [18].

With this introduction, the student is asked to use the *Dispersion Analysis* module of P.A.M.E.L.A to vary different parameters of the structure (waveguide width a and height D, dielectric substrate permittivity ε_r, strip position X_1 and width W…), trying to control the leakage constant of the leaky-mode without affecting its phase constant. The first question is to choose which leaky-wave mode is best suited to be used as the radiation mechanism of a practical LWA. In the strip-loaded dielectric LWA, three different modes were found (see Fig.9), namely the quasi static, the channel and the perturbed TE_{10} mode, in order of appearance. Their propagation constant frequency dispersion is plotted in Fig.17.

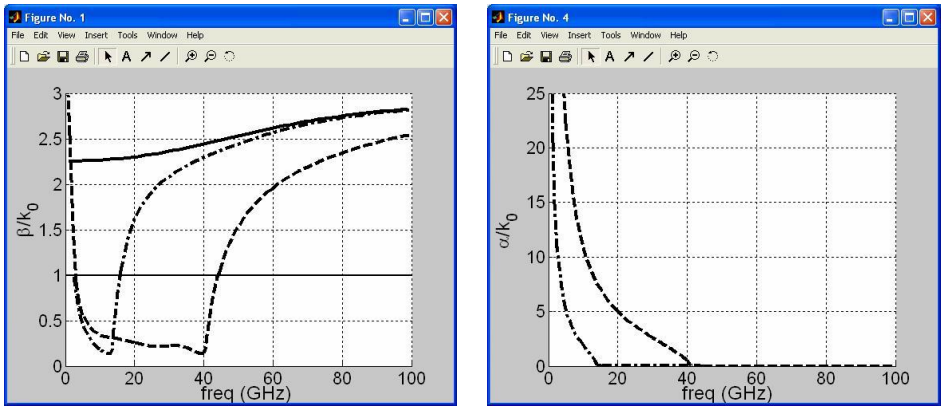

Fig. 17. Frequency dispersion of the propagation constants of the different modes in the strip-loaded LWA.

The quasi static mode is the main mode of the open waveguide. It can be seen from Fig.17 (continuous line) that its normalized phase constant β_y/k_0 is always greater than unity. Therefore, this mode cannot radiate, and must be avoided for uniform antenna applications. For this reason, the strip was connected to the side wall, making this mode to disappear from the modal spectrum of the waveguide. The other two modes have a radiation range. The dominant leaky-wave mode is the channel guide mode (dotted-dashed line), while the second leaky-wave mode to appear is the perturbation of the TE_{10} mode (dashed line). Although the two modes radiate in their corresponding radiation band (around *17GHz* and *43GHz*, as it can be seen in Fig.17 from the range corresponding to Eq.(11)), the TE_{10} mode is more suited to be used in antenna applications than the channel guide. The reason is that the TE_{10} mode radiation can be better controlled (vary α_y without changing β_y). This is due to the fact that the channel guide excites the main PPM ($m=0$) independently of the strip position or width, since the net electric field of the channel guide is directed from one side wall to the other (horizontal electric field), as could be seen in Fig.9-2. In opposition, the TE_{10}

mode is vertically polarized, and must be asymmetrically perturbed to excite the main PPM (*m=0*), as it was shown in Fig.13-a and 13-b. In this way, by controlling the strip position or width, the leakage rate can be controlled from zero (when the strip is symmetrically located) to high values (for a high degree of asymmetry). This control is not possible for the channel guide mode. It can therefore be said that the TE_{10} mode allows to control the radiation rate by the asymmetry principle, while the channel guide does not.

With this third exercise, the student must have learnt the next concepts:

1) A versatile LWA design is based on radiation from a leaky-wave mode, whose phase and leakage constants can be controlled independently.
2) For this purpose, the different types of open waveguide must be examined to find a geometrical parameter of its cross section which can perform the aforementioned control of the radiation.
3) Moreover, not all the leaky-wave modes of a given open waveguide can be controlled in the same way. For instance, the perturbed TE_{10} mode of a dielectric guide is better suited for antenna applications than a channel-guide mode.

VII. PERIODIC LEAKY-WAVE ANTENNAS: EXCITATION OF SPACE HARMONICS

The second basic type of LWA is based on periodic structures, sharing some similarities, but also having some differences, with respect to uniform LWA [6]. PAMELA environment allows to analyze periodically perturbed dielectric guides, by just introducing in the *Input Parameter* window (Fig.5) different values for the unit cell length (parameter *P* in Fig.1-c) and for the strip or slot length (parameter *Q*). In this example, the parameters of the proposed periodical strip-loaded guide are: *P=3.38mm*, *Q=2.366mm*, *L=1mm*, *D=1.4mm*, *H=0mm*, ε_r*=9mm*, *W=0.84mm*, *f=42GHz*, which are those of a practical published design [19]. The student must be introduced to the basic theory of ***Space Harmonics*** before the practical session [20].

When the cross section of a structure is no more uniform but instead it is of periodic nature, it cannot be properly said that the modal solution of such structures is described by the given modal longitudinal wavenumber. However, it can be said that the solutions of a periodical structure can be expressed by an infinite summation of space harmonics, the phase constant of all of them being related with the next expression:

$$\beta_{yn} = \beta_{y0} + n\frac{2\pi}{P} \qquad n=-\infty, .. ,-2,-1,0,+1,+2, .. ,+\infty \tag{14}$$

being *P* the period of the structure (length of the unit cell). Once the phase constant of the main space harmonic ($n=0 \rightarrow \beta_{y0}$) is known, the propagation constant of the set of higher-order space harmonics can be determined by Eq.(14). In this way, it can be said that the main space harmonic wavenumber value is a representative solution for the periodical structure, as it is done for the modal solutions of a uniform guide.

The student is asked to study the closed periodical structure, by computing the *detP* function sweeping ε_{reff} from *-9* to *9*, since the substrate relative permittivity is $\varepsilon_r=9$ (we will explain later the physical meaning of having negative values for β_y and ε_{reff}) . Once the Show Det-P button has been pressed and all the zeros are searched, the aspect of the main window detP graph obtained is shown in Fig.18.

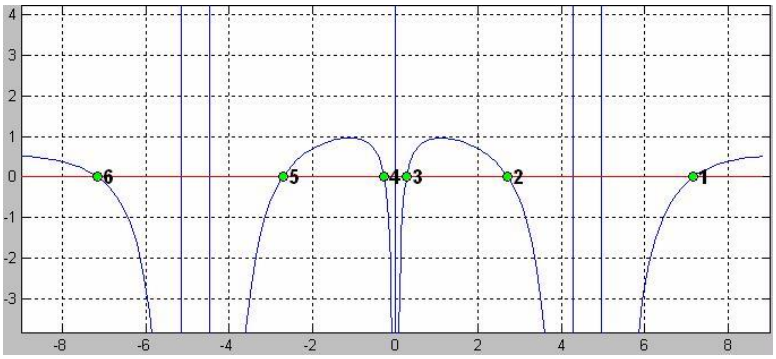

Fig. 18. *DetP* plot for the closed periodically strip-loaded dielectric guide (*42GHz*).

Six real solutions (six zeros of *DetP*) are found at the frequency of *42GHz* and between the proposed limits of ε_{reff}. However, the student must learn to interpret the physical meaning of these solutions. For this purpose, it is needed to make a new analysis at a different but close frequency and find again the zeros, in order to observe the frequency behavior of these solutions. Figure 19 shows the same plot of Fig.18, but having added the position of the zeros found at *40GHz*. The arrows indicate the evolution of the zeros in the increasing frequency direction, from *40GHz* to *42GHz*.

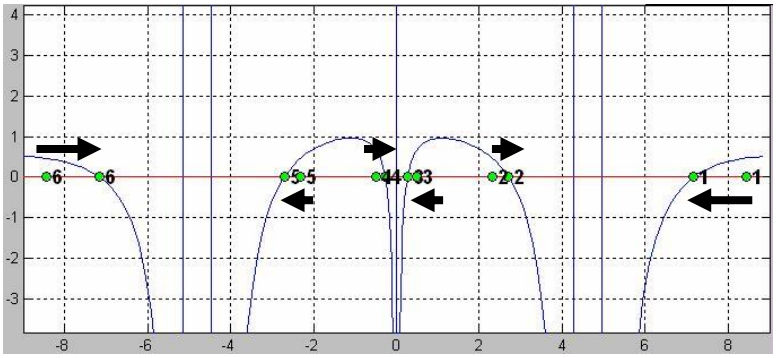

Fig. 19. Evolution with the frequency of the zeros for the periodic closed guide, from *40GHz* to *42GHz*.

At a first glance, the student could think that six different solutions exist in this periodical structure; however, all of them are related. The zeros found with numbers 2, 4 and 6 are related by Eq.(14), therefore being part of the same set of space harmonics. Mode 2 ($\beta_{y0}=+1275.2$ *rad/m*) is the main space harmonic, and modes 4 and 6 are the space harmonic of indexes *n=-1* and *n=-2* respectively:

$$\beta_{yn} = 1275.2 + n\frac{2\pi}{3.38}10^3 \quad \text{(rad/m)} \tag{15}$$

On the other hand, modes 1, 3 and 5 are also related by Eq.(14), which determines the space harmonic order of each one (mode 5 is *n=0*, mode 3 is *n=-1* and mode 1 is *n=-2*) :

$$\beta_{yn} = -\left(1275.2 + n\frac{2\pi}{3.38}10^3\right) \quad \text{(rad/m)} \tag{16}$$

Moreover, Eqs.(15) and (16) are related, since one equation is the other equation but with the sign changed. The student must remember that a given modal solution of inhomogeneous Maxwell's equations has two variants, the progressive and the regressive one, having their phase constants with the sign changed. The physical meaning of each solution is that of an ingoing or an outgoing wave, with respect to the selected waveguide direction (y-direction in our case). The sign of the power flow direction of a wave can be computed with the next expression related to the group velocity [2] (slope of the β-ω dispersion diagram):

$$PowerFlowDirection = sign\left(\frac{\partial\beta_y}{\partial\omega}\right)\cdot\hat{y} \tag{17}$$

From the frequency evolution shown in Fig.19, it is seen that, as expected, zeros with numbers 2, 4 and 6 correspond to the progressive space harmonic solution (+y direction), while zeros 1,3, and 5 are the solution of the corresponding regressive counterpart. The student must fix its attention on the progressive set of space harmonic solutions (zeros 2, 4 and 6). Some of them have a positive phase constant (mode 2 in Fig.18), while others have a negative phase constant (modes 4 and 6 in Fig.18). The sign of β_y indicates the direction of the phase change (related to the phase velocity). It is said that a propagating wave is a ***forward-wave*** if its group and phase velocities are parallel, while if they are antiparallel this wave is said to be a *backward-wave*. Table 1 summarizes all these concepts for the studied zeros.

Zero Number	***β_y solution @40GHz(rad/m)***	***Harmonic Index n***	***Power Flow Direction***	***Phase Change Direction***
2	+ 1275.2	n=0	Progressive, +y	Forward, +y
4	- 582.6	n=-1	Progressive, +y	Backward, -y
6	- 2433.9	n=-2	Progressive, +y	Backward, -y
1	+ 2433.9	n=-2	Regressive, -y	Backward, +y
3	+ 582.6	n=-1	Regressive, -y	Backward, +y
5	-1275.2	n=0	Regressive, -y	Forward, -y

Table 1. Classification of the zeros found in Fig.18.

The existence of backward waves is a very interesting phenomenon, known for many years [6, 20, 21], which now has obtained much interest in the scientific community due to the attractive and practical applications of ***metamaterials*** [22]. PAMELA tool helps to understand this interesting phenomenon of backward waves, and the application of ***backward leaky-wave modes*** to LWA [23-24]. As done for uniform

open waveguides, the radiation region of a mode in an open periodical waveguide can be determined with the next equation, which is an extension of Eq.(8) for the case in which negative phase constants are allowed to exist (space harmonics):

$$-1 < \frac{\beta_{yn}}{k_0} < +1 \tag{18}$$

This last expression is the key formula of radiation from open periodical structures. If any space harmonic (β_{yn}) of a given solution is in the radiation region, the mode of the periodical open waveguide will radiate, having the set of space harmonic a complex solution, with an imaginary part (α_y) accounting for the radiation losses:

$$k_{yn} = \beta_{yn} - j\alpha_y = \beta_{y0} + n\frac{2\pi}{P} - j\alpha_y \tag{19}$$

Depending on the case, the radiating space harmonic can be a backward leaky-wave ($-1<\beta_{yn}/k_0<0$) or a forward leaky-wave ($0<\beta_{yn}/k_0<+1$). Equation 12 can also be extended to the radiation of any space harmonic, obtaining its elevation angle of maximum radiation:

$$sin\,\theta_{m,n} \cong \frac{\beta_{yn}}{k_0} \tag{20}$$

The user must obtain the frequency dispersion response for the leaky-wave mode using the zero with number 2 in Fig.18. This zero was associated to the main progressive space harmonic of the open periodical waveguide. The program automatically detects that the structure is periodical ($P \neq Q$) and obtains the set of space harmonics associated to this solution, using Eq.(19). Figure 20 shows the results obtained for the phase constants of each space harmonic and the angle of radiation -Eq.(20), for a frequency sweep from *25GHz* to *65GHz*.

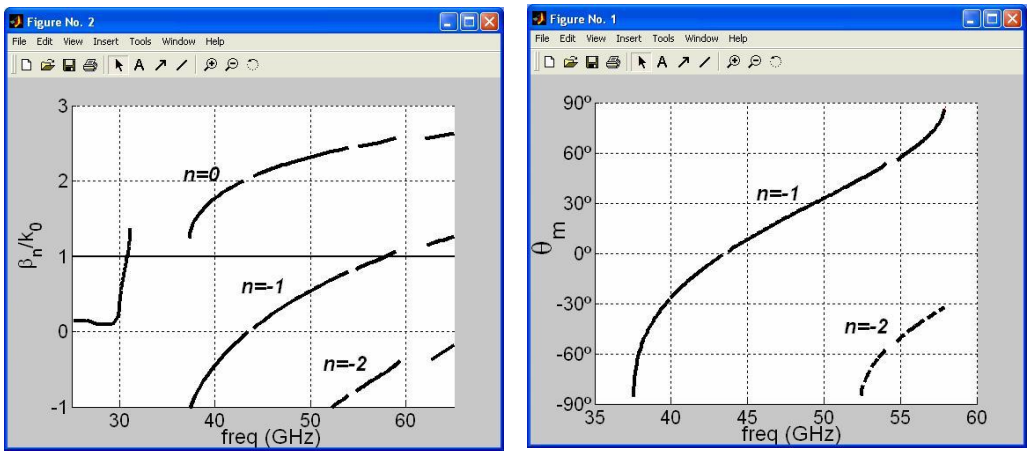

Fig. 20. Frequency dispersion of space harmonics phase constant and radiation angle.

Some interesting results can be obtained from Fig.20. The harmonics phase constants graph shows the evolution of *n=0,-1,-2* space harmonics. The main space harmonic curve resembles the dispersion of the phase constant of the waveguide mode, starting from closed to zero near the cut-off frequency (*30GHz*) and increasing its value with the frequency (as it corresponds to a progressive wave, see Eq.(17)). Therefore, the radiation region of this main space harmonic is always in the forward quadrant ($\beta_0/k_0>1$). In opposition, the *n=-1* space harmonic emerges from the backward-leaky zone at *38GHz* ($(\beta_{-1}/k_0>1 \rightarrow \theta_{m-1}<0^o)$) and crosses the forward-leaky region up to *58GHz* frequency, where this harmonic converts to a surface-wave. The second-order space harmonic behaves in a similar manner. The backward-to-forward scanning radiation mechanism of periodic LWA is represented in Fig.21-a, and can be easily understood from the last results. As in the uniform LWA, the traveling wave nature of the antenna provides a frequency-scanning behavior with frequency. The main difference is that the periodic perturbation allows to excite the *n=-1* harmonic, which can scan from backward to forward as the frequency is increased. The phase constant of the *n=-1* harmonic (β_{y-1}), changes it sign from negative (backward) to positive (forward), but the power direction inside the guide is always positive ($\partial\beta_{y-1}/\partial\omega>0$). However, the radiated beam is backward directed when the wave phase velocity is negative ($\beta_{y-1}<0$), due to the Fourier transform of such a backward illumination. The objective is to design the open waveguide dimensions and the periodic perturbations to make the *n=-1* space harmonic radiate in the desired frequency band.

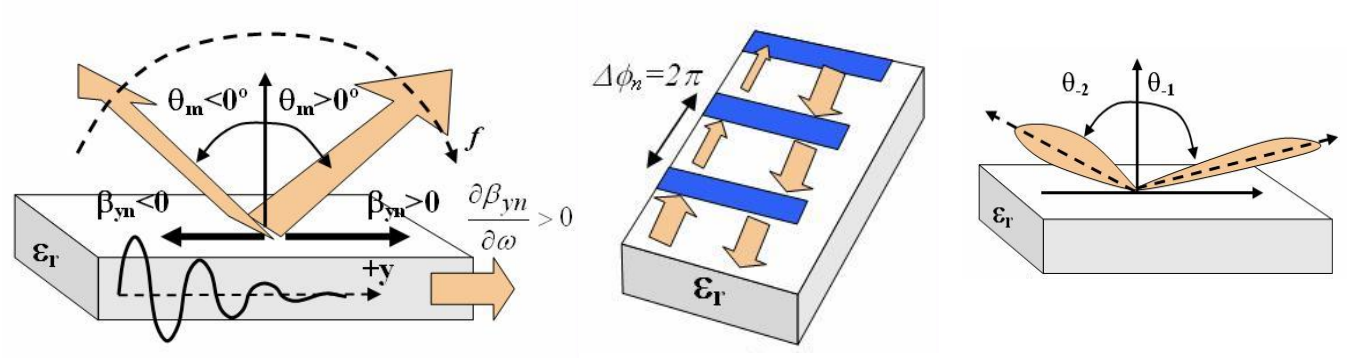

Fig. 21. a) Backward-to-forward scanning phenomenon. b) Band-gap phenomenon c) Multi-harmonic radiation

However, there are some frequency bands in which the phase constant seems to vanish. These zones are called ***prohibited band gaps***, and are common to all periodical structures, as the photonic crystals [25] or the frequency selective surfaces [26]. In these frequency bands, a reactive phenomenon occurs, therefore avoiding its propagation along the periodic structure. This phenomenon can be a desired effect in some applications, for instance in avoiding the excitation of surface waves in antenna applications, or when we want to reject the propagation of waves in some specified directions of the structure. However, in our case, the band gaps are an unwanted effect, which does not allow the antenna to radiate at some specific frequencies.

In Fig.20, a band gap appears at *44GHz*, in the broadside radiation direction of *n=-1* space harmonic. Another band gap is observed at *54GHz*. Figure 22 shows the value of the normalized attenuation constant α_y/k_0 of this leaky-wave mode. It can be seen a rapid raise in the value of α_y at the aforementioned band gap frequencies. As happened to leaky-wave modes below cut-off, this high value of α_y is not due to an increase of the radiation losses, but to a reactive rejection of the signal.

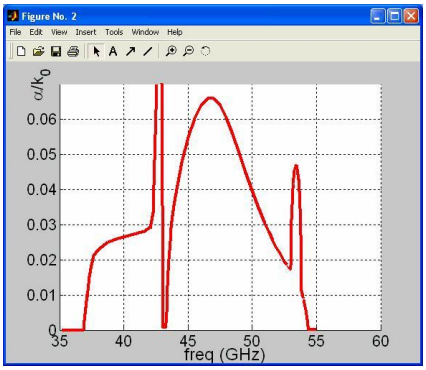

Fig. 22. Normalized attenuation constant for leaky-wave mode in open periodical waveguide, showing the rapid rise of α_y in the band gap regions.

This reactive behavior of the wave can be explained by a simple destructive interference phenomenon, illustrated in Fig.21-b [27]. The progressive wave incident in the strip is partially reflected back towards the source at each strip. Due to the fact that the distance between adjacent strips is *P*, the phase difference of an n-order space harmonic reflected back from a strip to the previous one can be computed as:

$$\Delta\phi_n = \beta_n \cdot P = \left(\beta_0 + n\frac{2\pi}{P}\right)\cdot P = \beta_0 \cdot P + n \cdot 2\pi \quad \text{(rad)} \tag{21}$$

When the $\Delta\phi$ is multiple of π, the reflected waves from each strip add in phase, creating a maximum of power reflected to the source, and therefore rapidly attenuating the resulting wave as it propagates along the structure in the progressive direction. The whole process is represented in Fig.21-b. From Eq.(21), it is easily obtained that one of the band gaps occurs when the antenna is scanning at broadside ($\beta_{-1}=0$), which corresponds to a value of $\beta_0=-2\pi/P$. In this case Eq.(21) leads to a phase difference $\Delta\phi_{-1}=2\pi$. The same result ($\Delta\phi_n=2\pi$) is obtained when any higher-order harmonic reaches the broadside direction. For this reason, this type of periodical leaky-wave antennas cannot scan in broadside. Some modifications must be made to allow the radiation in this direction [27].

A last important phenomenon is observed from Fig.20. It can be seen how the *n=-1* and the *n=-2* harmonics radiate at the same time above *52GHz*. Each space harmonic radiates a main narrow beam at its own elevation angle. This effect is illustrated in Fig.21-c, and is not desirable in many applications, since the multi-harmonic radiation can produce unwanted interferences. One important aspect in the design of a practical periodic LWA is to choose the period length (*P*) in order to avoid radiation from several harmonics. To understand this idea, the student must have in mind Eq.(14). For higher values of the period length *P*, the

spectral distance between consecutive harmonics is reduced. This can produce that a given higher-order harmonic reaches its radiation region (Eq.(18)) before the lower order harmonic has converted into a surface-wave. In practice, this reasoning is applied for the *n=0* and *n=-1* harmonics. Figure 23 shows the results obtained by varying *P* for a theoretical set of space harmonics in an ideal open rectangular waveguide, in which the main space harmonic would be obtained from the TE_{10} mode of the dielectric rectangular closed waveguide. In a real LWA design, the main space harmonic would be a perturbation of this TE_{10} mode. It can be seen that with *P=5mm*, the *n=-1* harmonic starts to radiate before the *n=0* harmonic has left the radiation region ($\beta_0/k_0<1$). As *P* is decreased, the *n=-1* harmonic moves away from the *n=0* curve. The same process is applied to obtain the maximum scanning angle of the *n=-1* harmonic, which is limited by the radiation of the *n=-2* harmonic. However, the period *P* cannot be made as small as desired, since it can produce that the first set of space harmonics (coming from the perturbed TE_{10} main mode) interfere with the next set of space harmonics (coming from the perturbed TE_{20} mode, for instance).

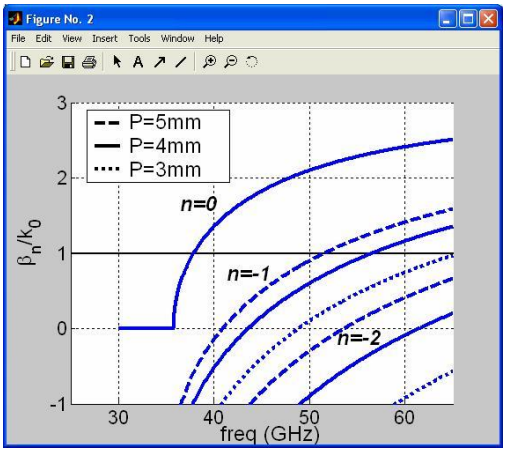

Fig. 23. Space harmonic curves obtained for different period lengths *P*. The results are obtained for the unperturbed TE_{10} mode of the closed dielectric guide.

The main concepts which must have been learnt by the student in these last exercises are summarized in the next points:

1) Periodic guides can be analyzed by using the space harmonic theory.
2) In the case of open periodic dielectric guides, any of the space harmonics must be in the radiation region to obtain a leaky-wave mode.
3) The main space harmonic (*n=0*) can radiate only in the forward quadrant. The *n=-1* harmonic can be used to frequency scan the radiated beam from backward to forward.
4) Prohibited band gaps occur at certain frequencies, in which the energy is reflected back to the source. One of these band gaps occurs at the broadside direction.
5) Much care must be taken with simultaneous radiation from different harmonics, which turns into the appearance of radiation lobes at different elevation angles. The election of the correct period dimension is important to determine the maximum and minimum scan-angles.

IX CONCLUSIONS

A software tool and associated GUI environment has been developed for the analysis of the modal spectrum of laterally-shielded rectangular open waveguides perturbed with planar metallizations. Due to its user-friendly interface, the input parameters can be easily introduced, and fast and visual results can be obtained in an interactive process. In this way, the user can learn many interesting concepts relating with leaky-waves. The program permits to analyze a high variety of structures to obtain the allowed spectrum of modes, including leaky-wave modes in radiating structures. Several examples have been presented to understand the nature of leakage in different types of waveguides. First, radiation from uniform waveguides has been illustrated using a strip loaded open dielectric rectangular waveguide. The surface-wave and the leaky-wave regimes have been studied, and the conditions to obtain radiation have been checked, introducing the necessity for the excitation of the main parallel-plate mode in its "fast-wave" region. Also the cut-off regime for leaky-waves has been revised, illustrating the difference between radiation losses (α^{RAD}) and reactive losses for evanescent cut-off complex waves (α^{REACT}). From the frequency dispersion curves for both β and α, the radiation characteristics (angle of maximum radiation θ_m and beamwidth $\Delta\theta$) of a given leaky-wave mode can be obtained, showing the frequency scanning capabilities of a uniform leaky-wave antenna, from near broadside to endfire. The second basic type of leaky-wave antenna is the periodically perturbed open waveguide. The concept of space harmonics is introduced; it is shown that an infinite number of solutions can be found, all of them being related by the period of the structure. By properly chosen the operation frequency, one can make the *n=-1* space harmonic to radiate from the backward direction to the forward one. In this way, the student has also been introduced to the interesting topic of left-handed propagation and metamaterials. The proposed software is being used in different courses at the Faculty of Telecommunication Engineering in Cartagena (Electromagnetic Field lab. -2nd course-, Microwave Engineering lab. -4th course-, and Advance Antenna Design course -Ph.D course-). This tool has also been used at the Technical University of Valencia, as part of the invited Ph.D. courses. To the authors' knowledge, this is the only tool specifically designed for helping in the teaching of leaky-wave modes. The results so far obtained (enquiries to the students and exams) assess that the method is succeeding to help the teachers and students in the knowledge of the complex topics of leaky-waves and backward radiation. The readers can find a free, stand-alone, executable version of PAMELA in the following link: http://www.tic.upct/html/investigacion/geat.

REFERENCES

[1] N. Marcuvitz, *Waveguide Handbook*, New York: McGraw-Hill, 1951.
[2] R.E. Collin, *Field Theory of Guided Waves*, New York: McGraw-Hill, 1960.
[3] T. Rozzi and M. Mongiardo, *Open Electromagnetic Waveguides*, IEE Electromagnetic Waves Series, vol. 43, 1997.
[4] A.A. Oliner, "Physical Description of Parasitic Mode Effects and Their Influence on Crosstalk and Package Effects", Proc. Workshop on Loss, Crosstalk and Package Effects in Microwave and Milimeter-Wave Integrated Circuits, *1991 IEEE MTT-S Int. Microwave Symp. Dig*.
[5] H. Shigesawa and M. Tsuji, "Leaky-Wave Phenomena and Their Unfavorable Effect in Millimeter-Wave Circuit Devices", *Microwave Conference*, 2001 APMC, vol.1, pp. 53-58, 2001.
[6] A.A. Oliner, Leaky-wave antennas, R.C. Johnson, *Antenna Engineering Handbook*, 3 rd ed, New York, McGraw-Hill, 1993, Ch. 10.
[7] N. Marcuvitz, "On field representation in terms of leaky modes", *IRE Trans.*, vol. AP-4, pp. 192-194, 1956.
[8] T. Tamir, "Inhomogeneous Waves Types at Planar Interfaces: III-Leaky Waves", *OPTIK*, Vol. 38,Nº 3,pp. 269-297, February 1973.
[9] W. Menzel, "A New Travelling-Wave Antenna in Microstrip", *Arch. Elekr. Uebertrag Tech.*, Vol. 33, pp. 137-140, April 1979.
[10] A.A. Oliner, "Leakage from higher modes on microstrip line with application to antennas", *Radio Sci.*, vol. 22, Nº 6, pp. 907-912, November 1987.
[11] K.C. Gupta, T. Itoh and A.A. Oliner, "Microwave and RF Education- Past, Present, and Future", *IEEE Trans. Microwave Theory Tech.*, Vol. 50, No.3, pp. 1006-1014, March 2002.
[12] J.L. Gómez and A.A. Melcón, "Non-Orthogonality Relations between Complex-Hybrid-Modes: an Application for the Leaky-Wave Analysis of Laterally-Shielded Top-Open Planar Transmission Lines", *IEEE Trans. Microwave Theory Tech*., Vol. 52, No.3, pp. 760-767, March 2004.
[13] J.L. Gómez and A.A. Melcón, "Radiation Analysis in the Space Domain of Laterally-Shielded Planar Transmission Lines. Part I: Theory", *Radio Science*, Vol.39, No.3, pp.1-11, June 2004.
[14] H. Shigesawa, M. Tsuji, P. Lampariello, F. Frezza and A. A. Oliner, "Coupling between different leaky-mode types in stub-loaded leaky waveguides", *IEEE Trans. Microwave Theory Tech*., Vol. 42, pp. 1548-1560, August 1994.
[15] J.L. Gómez, A.A. Melcón and F.D. Quesada, "A Full-Wave Space-Domain Method for the Analysis of Leaky-Wave modes in Multilayered Planar Open Parallel-Plate Waveguides", *International Journal of RF and Microwave Computer-Aided Engineering*, Vol.15, No.1, pp.128-139, January 2005.
[16] P. Lampariello, F. Frezza and A.A. Oliner, "The Transition Region Between Bound-Wave and Leaky-Wave Ranges for a Partially Dielectric-Loaded Open Guiding Structure", *IEEE Trans. Microwave Theory and Tech.*, Vol. 38, No 12, pp. 1831-1836, December 1990.
[17] J.L. Gómez and A.A. Melcón, "Radiation Analysis in the Space Domain of Laterally-Shielded Planar Transmission Lines. Part II: Applications", *Radio Science*, Vol.39, No.3, pp.12-22, June 2004.
[18] J.L. Gómez , A. de la Torre, D. Cañete, M. Gugliemi and A.A. Melcón, "Design of Tapered Leaky-Wave Antennas in Hybrid Waveguide-Planar Technology for Millimeter Waveband Applications", *IEEE Trans. Antennas Propagat.*, Vol.53, No.8, pp.2563-2577, August 2005.
[19] M. Guglielmi and G. Boccalone, "A Novel Theory for Dielectric-Inset Waveguide Leaky-Wave Antennas", *IEEE Trans. Antennas Propagat.*, Vol.49, pp. 497-504, 1991
[20] F. Schwering and S.T. Peng, "Design of Dielectric Grating Antennas for Millimeter-Wave Applications", *IEEE Trans. Microwave Theory Techn.*, Vol.31, pp. 199-209, February 1983.

[21] V.G. Veselago, "Electrodynamics of Substances with Simulataneously Negativevalues of mu and epsilon", *Soviet Physics Uspekhi*, Vol. 10, pp. 509-514, January-February 1968.
[22] D.R. Smith, W.J. Padilla, D.C. Vier, R. Shelby, S.C. Nemat-Nasser, N. Kroll and S. Schultz, "Left Handed Metamaterials", *Photonic Crystals and Light Focalization*, Costas M. Soukoulis Ed. (Kluwer Academic, Dordrecht, 2001), p.351., 2001.
[23] A. Grbic and G.V. Eleftheriades, "Experimental Verification of Backward-Wave Radiation from a Negative Refractive Index Metamaterial", *Journal of Applied Physics*, Vol.92, pp. 5930-5935, November 2002.
[24] L. Liu, C. Caloz and T. Itoh, "Dominant Mode (DM) Leaky Wave Antenna with Backfire-to-Endfire Scanning Capabilty", *Electron. Lett.*, Vol. 38, No. 23, pp. 1414-1416, November 2002.
[25] L. Brillouin, *Wave Propagation in Periodic Structures: Electric Filters and Crystal Lattices*, Ed. McGraw Hill, New York, 1946; Dover Publications, New York, 1953.
[26] B.A. Munk, *Frequency Selective Surfaces: Theory and Design*, Ed. John Wiley & Sons, 2000, ISBN 0-471-37047-9.
[27] M. Guglielmi and D.R. Jackson, "Broadside Radiation from Periodic Leaky-Wave Antennas", *IEEE Trans. Antennas Propagat.*, Vol. 41, No.1, pp. 31-37, Jan. 1993.